SCIENTIFIC REPORTS

OPEN

SUBJECT AREAS:
UBIQUITINS
NEURAL STEM CELLS
GLIOGENESIS
GROWTH FACTOR SIGNALLING

Received
15 September 2014

Accepted
29 October 2014

Published
13 November 2014

Correspondence and requests for materials should be addressed to K.-Y.R. (kyryu@uos.ac.kr)

Disruption of polyubiquitin gene *Ubb* causes dysregulation of neural stem cell differentiation with premature gliogenesis

Han-Wook Ryu, Chul-Woo Park & Kwon-Yul Ryu

Department of Life Science, University of Seoul, Seoul 130-743, Republic of Korea.

Disruption of polyubiquitin gene *Ubb* leads to early-onset reactive gliosis and adult-onset hypothalamic neurodegeneration in mice. However, it remains unknown why reduced levels of ubiquitin (Ub) due to loss of *Ubb* lead to these neural phenotypes. To determine whether or not the defects in neurons or their progenitors *per se*, but not in their cellular microenvironment, are the cause of the neural phenotypes observed in $Ubb^{-/-}$ mice, we investigated the properties of cultured cells isolated from $Ubb^{-/-}$ mouse embryonic brains. Although cells were cultured under conditions promoting neuronal growth, $Ubb^{-/-}$ cells underwent apoptosis during culture *in vitro*, with increased numbers of glial cells and decreased numbers of neurons. Intriguingly, at the beginning of the $Ubb^{-/-}$ cell culture, the number of neural stem cells (NSCs) significantly decreased due to their reduced proliferation and their premature differentiation into glial cells. Furthermore, upregulation of Notch target genes due to increased steady-state levels of Notch intracellular domain (NICD) led to the dramatic reduction of proneuronal gene expression in $Ubb^{-/-}$ cells, resulting in inhibition of neurogenesis and promotion of gliogenesis. Therefore, our study suggests an unprecedented role for cellular Ub pools in determining the fate and self-renewal of NSCs.

Post-translational modification of proteins via ubiquitin (Ub) is known to play diverse functions, including proteasomal degradation, regulation of signal transduction pathways, and endocytosis[1–3]. Since the discovery that neuron-specific protein gene product 9.5 (PGP9.5) is a Ub C-terminal hydrolase L1[4], ubiquitylation has also been shown to play a pivotal role in embryonic neural development[5] and in neuronal function and dysfunction[6], both of which require precise control of signaling pathways. In fact, ubiquitylation has been shown to be an essential process in neurogenesis, neuritogenesis, and synaptogenesis, and several E3 ligases, along with their specific substrates, have been identified in these processes[5]. However, the effect of reduced ubiquitylation of these substrates during neural development has not been elucidated.

We previously demonstrated that reduced levels of Ub due to loss of polyubiquitin gene *Ubb* leads to two striking neural phenotypes: adult-onset hypothalamic neurodegeneration and early-onset reactive gliosis[7,8]. Usually, neurodegeneration accompanies reactive gliosis, whereas in $Ubb^{-/-}$ mice, reactive gliosis precedes neurodegeneration in the hypothalamus. However, it remains unknown why reduced levels of Ub lead to reactive gliosis, and it is unclear whether the defects reside in neurons or their progenitors *per se*, but not in their cellular microenvironment. To identify the exact cause of $Ubb^{-/-}$ neural phenotypes, we cultured cells isolated from embryonic brains to determine the presence of neuronal or neural stem/progenitor cell autonomous defects upon *Ubb* disruption.

During brain development, neural stem cells (NSCs) or progenitors generate neuroblasts and glioblasts, which differentiate into neurons and glial cells, such as astrocytes and oligodendrocytes, respectively[9–11]. The timing of these cell generation processes is important in the construction of normal brain cytoarchitecture, and it is well known that neurogenesis precedes gliogenesis[12]. Usually, neurogenesis occurs during mid-gestation and ends at birth, whereas gliogenesis occurs mostly after birth[13]. One of the key regulators of this switch during NSC differentiation is Notch signaling[14,15]. Notch signaling is downregulated to promote neurogenesis in the embryonic stage, and conversely, Notch signaling is upregulated to promote gliogenesis and maturation of neurons in the postnatal stage. In addition to the timed control of NSC differentiation, maintenance or self-renewal of NSCs has also been shown to be important for proper neural development[16].

Here, we demonstrate that NSC numbers were reduced in *Ubb*$^{-/-}$ cells while glial cell numbers increased due to reduced proliferation of NSCs and to the dysregulated timing of gliogenesis. We hypothesize that NSCs in *Ubb*$^{-/-}$ mouse brains acquired higher gliogenic potential than neurogenic potential, meaning that gliogenesis occurred prematurely. Therefore, our data show that cellular Ub levels are important determinants in controlling the fate and timing of NSC differentiation into neurons and glial cells, and cellular Ub levels also affect self-renewal of NSCs.

Results

Reduced survival and increased apoptosis in *Ubb*$^{-/-}$ cells isolated from embryonic brains. Cells were isolated from embryonic brains on 14.5 dpc (days post coitum) and cultured in medium to promote neuronal growth while suppressing growth of glial cells, such as astrocytes. Cultured wild-type cells displayed properties typical of neurons but not glial cells, as they were positive for the neuronal markers βIII-tubulin (TUJ1) and neuronal nuclei (NeuN), while negative for the astrocyte marker glial fibrillary acidic protein (GFAP) (Fig. 1a and 1b). On the other hand, cells were positive for GFAP and negative for TUJ1 and NeuN when cultured in medium that promotes glial cell growth (Fig. 1a and 1b). Therefore, cells were cultured in neuronal growth medium throughout the study.

Since *Ubb*$^{-/-}$ mice are born smaller than their wild-type littermates[8], the brains of *Ubb*$^{-/-}$ embryos were also smaller than those of wild-type embryos on most occasions (unpublished observation). Accordingly, the total cell number obtained from *Ubb*$^{-/-}$ embryonic brains was about 70% compared to wild-type on 14.5 dpc (Fig. 1c). Although we plated the same number of cells from wild-type and *Ubb*$^{-/-}$ embryonic brains, the intensity of NeuN-immunoreactive bands in the lysates of *Ubb*$^{-/-}$ cells cultured *in vitro* for 13 days was about 65% compared to wild-type cells (Fig. 1b). Therefore, we monitored the number of cells during the culture period. The total number of *Ubb*$^{-/-}$ cells continuously decreased during culture, whereas the number of wild-type cells was maintained (Fig. 1d).

To determine whether or not the gradual reduction of *Ubb*$^{-/-}$ cells during culture can be attributed to increased apoptosis, we performed TUNEL assay using cells cultured *in vitro* for 3 days, just before we observe the reduction of *Ubb*$^{-/-}$ cells. Although TUNEL^{+} cells were hardly observed in wild-type cells, one third of *Ubb*$^{-/-}$ cells were TUNEL^{+} (Fig. 2a). Thus, it is evident that the reduction in *Ubb*$^{-/-}$ cells was due to increased apoptosis. To identify *Ubb*$^{-/-}$ cell

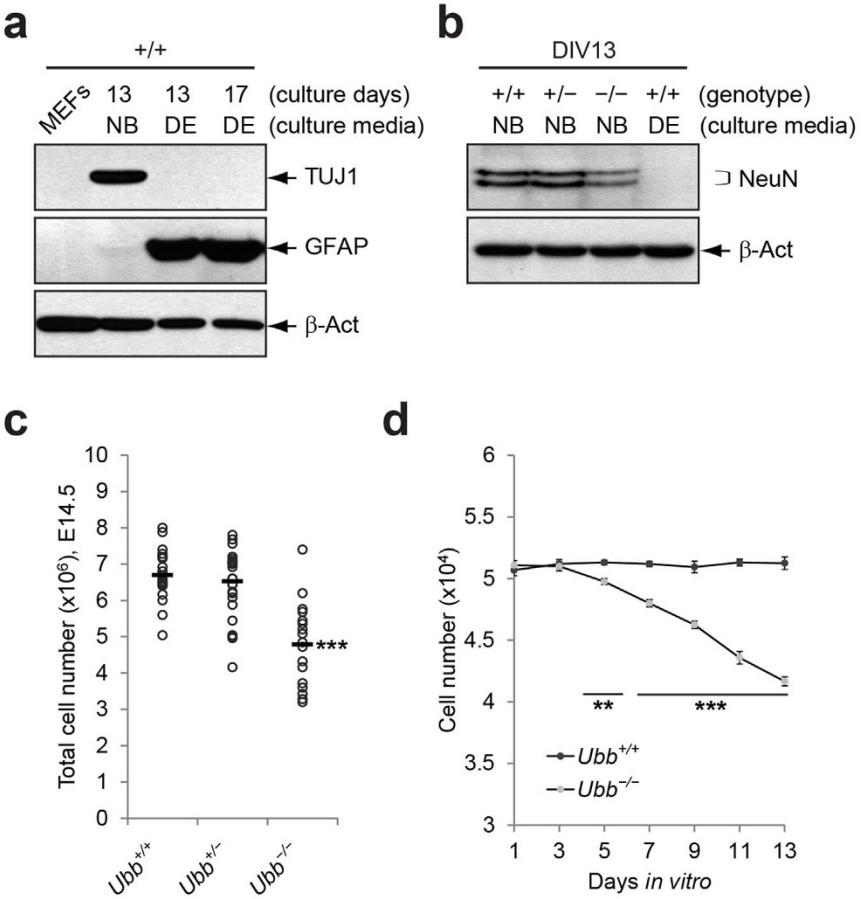

Figure 1 | Reduced number of *Ubb*$^{-/-}$ cells during culture *in vitro*. (a) Immunoblot detection of neuronal marker TUJ1 and glial cell marker GFAP in cells isolated from wild-type (+/+) embryonic brains on 14.5 dpc that were cultured under two different medium conditions. Growth of neurons was facilitated in Neurobasal® medium with B-27 supplement (NB), whereas growth of glial cells was preferred in DMEM/10% FBS (DE). β-Actin (β-Act) was used as a loading control, and mouse embryonic fibroblasts (MEFs) were included as a negative control. (b) Immunoblot detection of neuronal marker NeuN at 48 and 46 kDa in cells isolated from wild-type (+/+), *Ubb*$^{+/-}$ (+/−), and *Ubb*$^{-/-}$ (−/−) embryonic brains on 14.5 dpc and cultured *in vitro* for 13 days (DIV13). Wild-type (+/+) cells were cultured in two different medium conditions (NB and DE). (c) Determination of total cell numbers in *Ubb*$^{+/+}$ ($n = 19$), *Ubb*$^{+/-}$ ($n = 25$), and *Ubb*$^{-/-}$ ($n = 17$) embryonic brains on 14.5 dpc. (d) Cells isolated from *Ubb*$^{+/+}$ ($n = 4$) and *Ubb*$^{-/-}$ ($n = 3$) embryonic brains were plated on 96-well plate at 5×10^4 cells/well and cultured *in vitro* and counted using a hematocytometer. Representative immunoblot results of cells from two different embryonic brains per genotype are shown (a, b), and data are expressed as the means ± SEM from the indicated number of samples (c, d). $^{**}P < 0.01$; $^{***}P < 0.001$ *vs.* *Ubb*$^{+/+}$ (c) or *Ubb*$^{+/+}$ on each day (d).

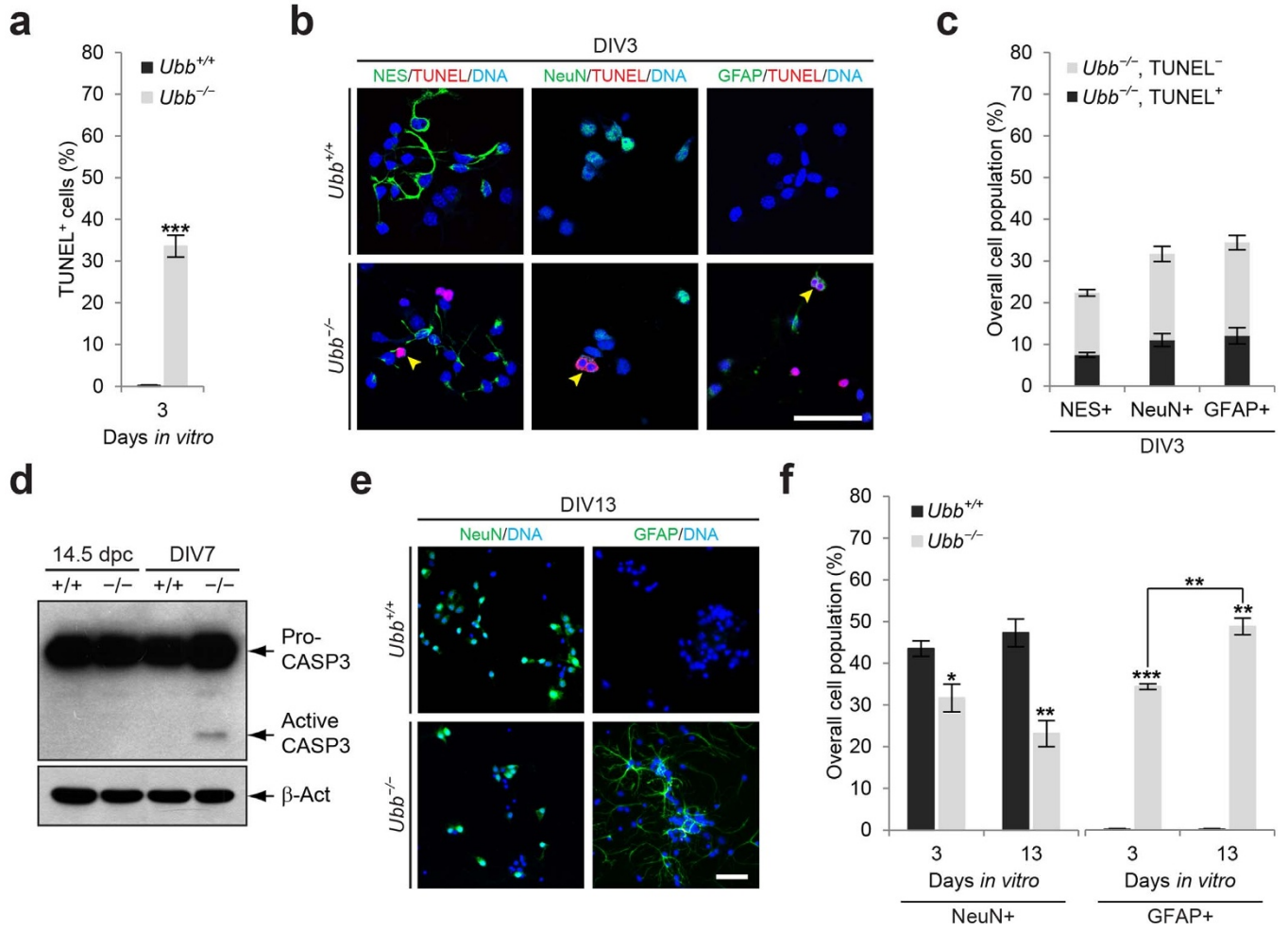

Figure 2 | Increased apoptosis in *Ubb*$^{-/-}$ cells during culture *in vitro*. (a) Cells isolated from wild-type (*Ubb*$^{+/+}$) and *Ubb*$^{-/-}$ embryonic brains ($n = 3$ each) on 14.5 dpc were cultured *in vitro* for 3 days. To determine the percentages of cells undergoing apoptosis, the total number of TUNEL$^+$ cells was divided by the total number of DAPI$^+$ cells in three randomly selected fields for each sample. For each sample, more than 100 DAPI$^+$ cells were counted. (b) Cells isolated from wild-type (*Ubb*$^{+/+}$) and *Ubb*$^{-/-}$ embryonic brains on 14.5 dpc and cultured *in vitro* for 3 days (DIV3) were subjected to a double-labeling fluorescence TUNEL assay with the NSC marker NES, neuronal marker NeuN, and glial cell marker GFAP, and DNA was visualized with DAPI. Arrowheads indicate TUNEL$^+$ apoptotic cells that are also positive for cell-type specific markers. (c) The percentage of apoptotic (TUNEL$^+$) or non-apoptotic (TUNEL$^-$) NES$^+$, NeuN$^+$, or GFAP$^+$ *Ubb*$^{-/-}$ cells ($n = 3$) was determined in a similar manner as described in (a). (d) Immunoblot detection of apoptotic marker caspase-3 (CASP3) in wild-type (+/+) and *Ubb*$^{-/-}$ (−/−) embryonic brain lysates on 14.5 dpc (14.5 dpc) or in cells isolated from embryonic brains on 14.5 dpc and cultured *in vitro* for 7 days (DIV7). CASP3-immunoreactive bands were detected at 35 and 17 kDa, representing pro-caspase-3 (pro-CASP3) and active caspase-3 (active CASP3). β-Actin (β-Act) was used as a loading control. (e) Wild-type (*Ubb*$^{+/+}$) and *Ubb*$^{-/-}$ cells on DIV13 were stained with markers for GFAP or NeuN, and DNA was visualized with DAPI. (f) On DIV3 and DIV13, the percentages of wild-type (*Ubb*$^{+/+}$) and *Ubb*$^{-/-}$ cells ($n = 3$ each) positive for NeuN or GFAP were determined in a similar manner as described in (a). Representative images or immunoblot results of cells from three different embryonic brains per genotype are shown (b, d, e), and data are expressed as the means ± SEM from the indicated number of samples (a, c, e). $^*P < 0.05$; $^{**}P < 0.01$; $^{***}P < 0.001$ *vs.* *Ubb*$^{+/+}$ on each day or as indicated by bars. Scale bars, 50 μm.

types that undergo apoptosis, cells cultured *in vitro* for 3 days were stained for GFAP, NeuN, or NSC marker nestin (NES) in combination with the TUNEL assay (Fig. 2b). Of the apoptotic cells (~34%), about 12% were GFAP$^+$, about 11% were NeuN$^+$, and about 8% were NES$^+$ (Fig. 2c). Non-apoptotic GFAP$^+$, NeuN$^+$, and NES$^+$ cells were 22%, 21%, and 15%, respectively. Therefore, due to deletion of *Ubb*, all cell types that we investigated underwent apoptosis to some extent. However, it is highly likely that apoptotic stress is promoted in *Ubb*$^{-/-}$ cells during culture *in vitro*, as there was no evidence of apoptotic cell death in *Ubb*$^{-/-}$ embryonic brains on 14.5 dpc (Fig. 2d). This result also supports our previous observation that the number of hypothalamic neurons is maintained in 1-month-old *Ubb*$^{-/-}$ mice, while it is reduced by about 30% in adult *Ubb*$^{-/-}$ mice[8].

Intriguingly, when *Ubb* was disrupted, the number of GFAP$^+$ astrocytes gradually increased during culture (Fig. 2e and 2f), suggesting that the number of proliferating GFAP$^+$ cells exceeds that of apoptotic GFAP$^+$ cells. It took for a week for newly attached GFAP$^+$ cells to obtain their distinguishable morphology of astrocytes when cultured in neuronal growth medium (see Fig. 2b and 2e). On the other hand, NeuN$^+$ neuronal populations in *Ubb*$^{-/-}$ cells remained significantly lower than those in wild-type cells throughout the culture period (Fig. 2e and 2f). Therefore, apoptosis in *Ubb*$^{-/-}$ cells may be closely associated with the increase in the number of glial cells.

Reduced neural stem cell numbers and dysregulation of their differentiation upon disruption of *Ubb*. As the phenotype of *Ubb*$^{-/-}$ cells was apparent on DIV3, defects in *Ubb*$^{-/-}$ cells might

already have been present at the beginning of culture. Of interest, expression levels of *Gfap*, but not *Fox3*, which was identified as *NeuN*[17], significantly increased in $Ubb^{-/-}$ cells from DIV7 to DIV13. Therefore, we investigated the dysregulation of NSC differentiation into neurons and glial cells, which is thought to be tightly controlled during embryonic brain development[12]. To determine whether disruption of *Ubb* affects NSC differentiation, we measured the percentage of NES^+ NSCs in a given cell population on DIV1 (Fig. 3a and 3b). To our surprise, the percentage of NES^+ NSCs significantly decreased in $Ubb^{-/-}$ cells, even on DIV1, accompanied by a significant decrease in $NeuN^+$ neurons, as well as by a significant increase in $GFAP^+$ glial cells (astrocytes) (Fig. 3a and 3b). Decreased number of NES^+ NSCs and increased number of $GFAP^+$ astrocytes were also evident in $Ubb^{-/-}$ embryonic brains on 14.5 dpc (Fig. 3d).

To determine whether the decreased number of NES^+ NSCs in $Ubb^{-/-}$ cells was due to the reduced proliferation of NSCs, cells were co-stained with a proliferation marker, phospho-histone 3 (PH3) (Fig. 3a). We observed a dramatic reduction in the proliferation of NSCs and a significant increase in the proliferation of astrocytes in $Ubb^{-/-}$ cells (Fig. 3a and 3c). These results suggest that NSC cell numbers are intrinsically low in $Ubb^{-/-}$ embryonic brains due to reduced capacity to self-renew or proliferate to maintain NSCs. In $NeuN^+$ neurons, genes related to neuronal maturation have been shown to be transcriptionally activated by acetylation of Lys14 in H3, which facilitates the phosphorylation of H3[18,19]. Therefore, the occasionally observed PH3 immunoreactivity in $NeuN^+$ neurons may not necessarily indicate the proliferation status of cells.

To further confirm these results, we measured the expression levels of *Nes*, *Fox3* (*NeuN*), and *Gfap* in cells isolated from embryonic brains on both 14.5 dpc (no culture *in vitro*; DIV0) and DIV1 using qRT-PCR (Fig. 3e). In accordance with the immunofluorescence results, expression levels of *Nes* and *Fox3* (*NeuN*) significantly decreased, while *Gfap* expression significantly increased in cells isolated from $Ubb^{-/-}$ embryonic brains on 14.5 dpc, even before the start of *in vitro* culture. Similar results were obtained when we measured the mRNA levels of *Nes*, *Fox3* (*NeuN*), and *Gfap* in embryonic brains on 14.5 dpc (Supplementary Fig. S1a). These results suggest

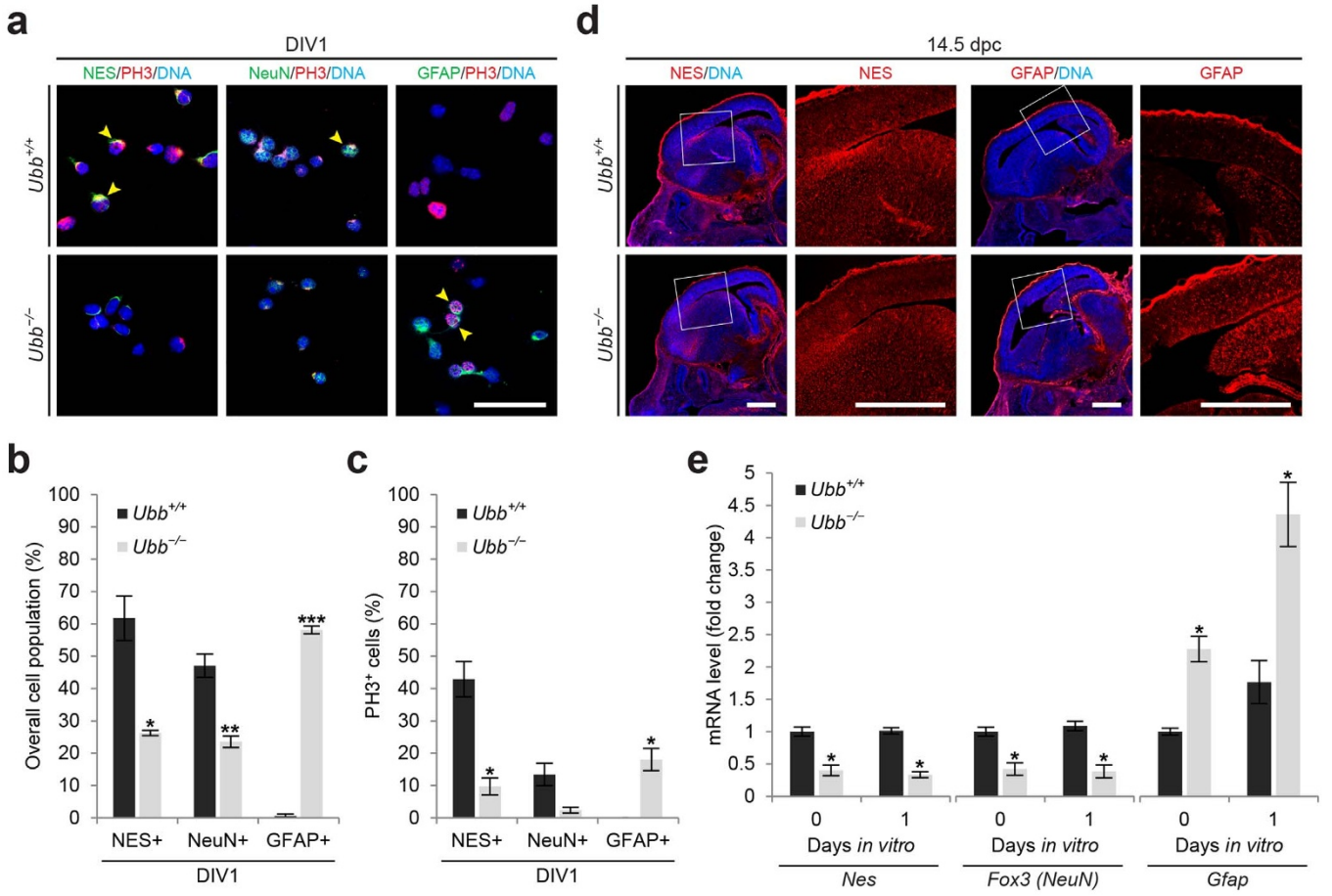

Figure 3 | Reduced number of neural stem cells and dysregulation of their differentiation in $Ubb^{-/-}$ cells. (a) Cells isolated from wild-type ($Ubb^{+/+}$) and $Ubb^{-/-}$ embryonic brains on 14.5 dpc and cultured *in vitro* for 1 day (DIV1) were stained with the NSC marker NES, neuronal marker NeuN, and glial cell marker GFAP in combination with a proliferation marker PH3, and DNA was visualized with DAPI. Arrowheads indicate $PH3^+$ cells that are also positive for cell-type specific markers. (b) On DIV1, the percentages of wild-type ($Ubb^{+/+}$) and $Ubb^{-/-}$ cells ($n = 3$ each) positive for NES, NeuN, or GFAP were determined in a similar manner as described in Figure 2(a). (c) On DIV1, the percentages of $PH3^+$ wild-type ($Ubb^{+/+}$) and $Ubb^{-/-}$ cells ($n = 3$ each) that were also positive for NES, NeuN, or GFAP were determined in a similar manner as described in Figure 2(a). (d) Frozen brain sections were prepared from wild-type ($Ubb^{+/+}$) and $Ubb^{-/-}$ embryos on 14.5 dpc and stained with the NSC marker NES and glial cell marker GFAP, and DNA was visualized with DAPI. (e) *Nes*, *Fox3* (*NeuN*), and *Gfap* mRNA levels in cells isolated from wild-type ($Ubb^{+/+}$) and $Ubb^{-/-}$ embryonic brains ($n = 3$ each) on 14.5 dpc (DIV0) or cultured *in vitro* for 1 day (DIV1) were determined by qRT-PCR and normalized to *Gapdh* levels. mRNA levels are expressed as a fold increase relative to wild-type levels on DIV0. Representative images of cells or sections from three different embryonic brains per genotype are shown (a, d), and data are expressed as the means ± SEM from the indicated number of samples (b, c, e). $*P < 0.05$; $**P < 0.01$; $***P < 0.001$ *vs.* $Ubb^{+/+}$ on each day. Scale bar for (a), 50 μm; scale bar for (d), 500 μm.

that differentiation of NSCs into neurons during mid-gestation was somehow inhibited, whereas premature NSC differentiation into glial cells occurred upon disruption of *Ubb*. This latter phenomenon is known to occur mostly after birth[13]. Therefore, the decrease in the number of NSCs in $Ubb^{-/-}$ embryonic brains can also be attributed to the dysregulation of NSC differentiation.

Uprgulation of Notch target genes in $Ubb^{-/-}$ cells due to increased steady-state levels of NICD. The timing of NSC differentiation into neurons (neurogenesis) or glial cells (gliogenesis) is controlled by Notch signaling. Specifically, differentiation into neurons is promoted by repression of Notch signaling during the mid-gestation period of embryonic development[15]. On the other hand, activation of Notch signaling after birth promotes differentiation into glial cells. Notch activation also supports the maturation of already differentiated neurons[15]. Therefore, we measured the expression levels of *Notch* along with its target genes in cells isolated from wild-type and $Ubb^{-/-}$ embryonic brains on both 14.5 dpc (DIV0) and DIV1. Expression levels of *Notch*, as well as its target genes, significantly increased in $Ubb^{-/-}$ cells (Fig. 4a), and remained high in $Ubb^{-/-}$ cells throughout the culture period (Fig. 4b). Similar results were obtained when we measured the mRNA levels of *Notch* and its target genes in embryonic brains on 14.5 dpc (Supplementary Fig. S1b).

To confirm that the upregulation of Notch target genes is indeed due to activation of Notch signaling in $Ubb^{-/-}$ cells, pharmacological intervention of Notch signaling using DAPT, a well-known inhibitor of γ-secretase, which indirectly inhibits Notch signaling by hampering cleavage of NICD, was exploited during culture *in vitro*. Upon treatment with DAPT, expression levels of *Notch*, as well as its target genes in $Ubb^{-/-}$ cells, decreased to those of wild-type cells (Fig. 4b). These results suggest that the upregulation of Notch target genes in $Ubb^{-/-}$ cells can be related to levels of cleaved NICD. To investigate this possibility, we measured the steady-state levels of Notch

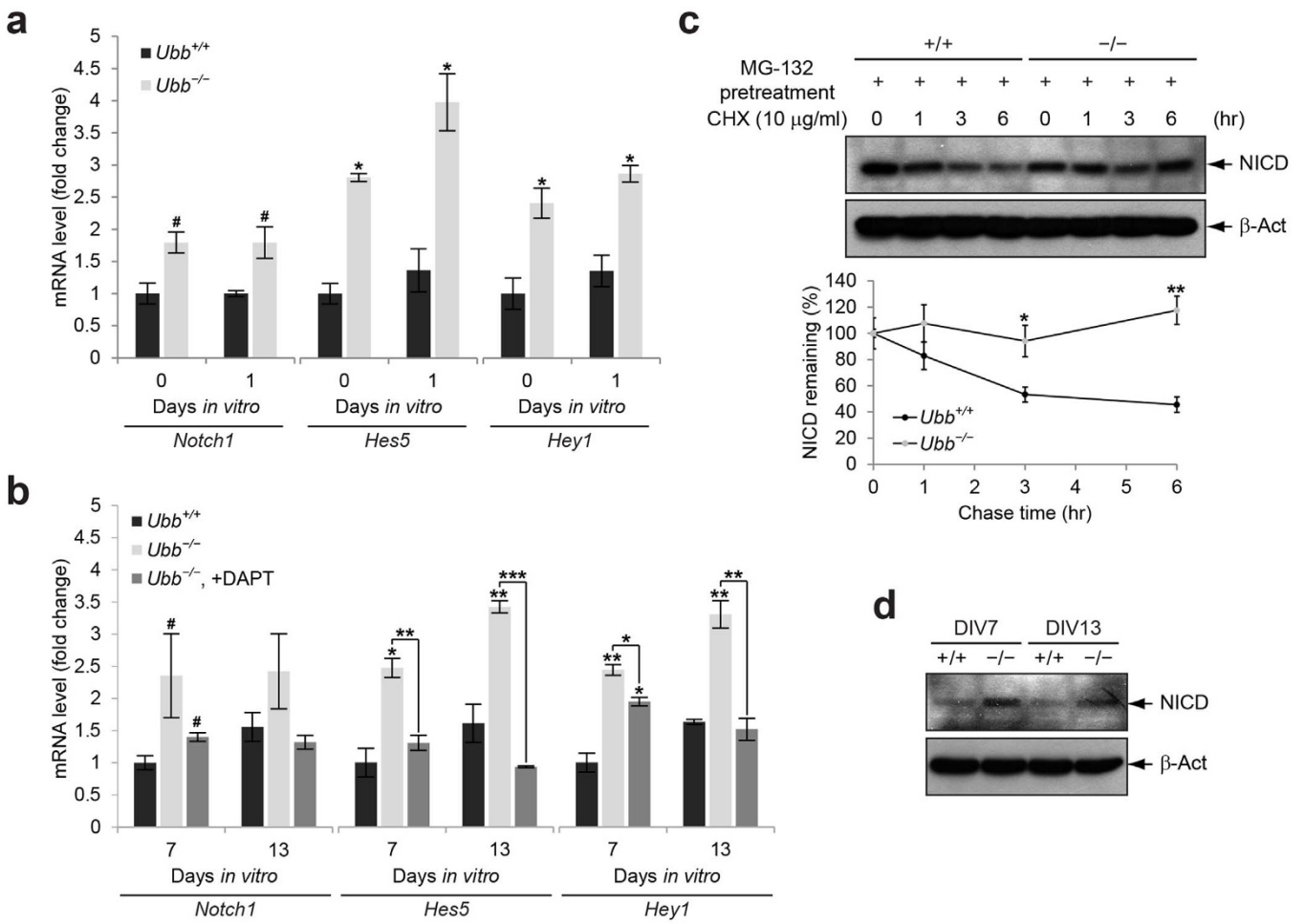

Figure 4 | Upregulation of Notch target genes and increased steady-state levels of NICD in $Ubb^{-/-}$ cells. (a) *Notch1*, *Hes5*, and *Hey1* mRNA levels in cells isolated from wild-type ($Ubb^{+/+}$) and $Ubb^{-/-}$ embryonic brains ($n = 3$ each) on 14.5 dpc (DIV0) or cultured *in vitro* for 1 day (DIV1) were determined by qRT-PCR and normalized to *Gapdh* levels. mRNA levels are expressed as a fold increase relative to wild-type levels on DIV0. (b) Expression levels of *Notch* and its target genes in wild-type ($Ubb^{+/+}$) and $Ubb^{-/-}$ cells ($n = 3$ each) on DIV7 and DIV13 were determined by qRT-PCR and normalized to *Gapdh* levels. mRNA levels are expressed as a fold increase relative to wild-type levels on DIV7. To repress Notch signaling, $Ubb^{-/-}$ cells cultured *in vitro* for 5 days (DIV5) were treated with 10 μM DAPT and cultured for another 2 to 8 days (DIV7 and DIV13). One-half of the medium containing 10 μM DAPT was changed every other day. (c) Cycloheximide (CHX) chase of stabilized NICD. Cells isolated from wild-type (+/+) and $Ubb^{-/-}$ (−/−) embryonic brains ($n = 3$ each) on 14.5 dpc and cultured *in vitro* for 7 days (DIV7) were pre-treated with 10 μM MG-132 for 2 hr to prevent degradation of NICD. Upon removal of MG-132, accumulated NICD was chased in medium containing 10 μg/ml CHX for up to 6 hr. β-Actin (β-Act) was used as a loading control. (d) Immunoblot detection of cleaved NICD in cells isolated from wild-type (+/+) and $Ubb^{-/-}$ (−/−) embryonic brains on 14.5 dpc and cultured *in vitro* for 7 and 13 days (DIV7 and DIV13). Representative immunoblot results of cells from three different embryonic brains per genotype are shown (c, d), and data are expressed as the means ± SEM from the indicated number of samples (a–c). $^{\#}P < 0.1$; $^{*}P < 0.05$; $^{**}P < 0.01$; $^{***}P < 0.001$ *vs.* $Ubb^{+/+}$ on each day or as indicated by bars.

intracellular domain (NICD), which was released following endocytosis of the Notch ligand Delta as well as the extracellular region of the Notch receptor in neighboring cells[20,21]. Increased steady-state levels of cleaved NICD were observed in *Ubb*$^{-/-}$ cells, probably due to the prolonged stabilization of NICD, which is usually rapidly degraded by the proteasome (Fig. 4c and 4d). Therefore, aberrant activation of Notch signaling in *Ubb*$^{-/-}$ cells is due to increased steady-state levels of NICD, although we cannot exclude the possibility that increased expression of *Notch* itself may also contribute to increased levels of NICD.

Aberrant activation of Notch signaling in *Ubb*$^{-/-}$ cells is linked to premature onset of gliogenesis and suppression of neurogenesis. Notch target genes *Hes5* and *Hey1*, which encode inhibitory basic helix-loop-helix (bHLH) transcription factors, are known to repress the function of proneuronal bHLH transcription factors encoded by proneuronal genes, such as *Neurog1*[22]. Neurogenins are required for activation of neuronal genes as well as neuronal differentiation. As expected, *Neurog1* expression levels were significantly reduced in *Ubb*$^{-/-}$ cells on DIV0 and DIV1, as well as in embryonic brains on 14.5 dpc (Fig. 5a and Supplementary Fig. S1c), and reduced *Neurog1* expression was also observed in *Ubb*$^{-/-}$ cells throughout the culture period (Fig. 5b). Therefore, reduced expression of proneuronal genes in *Ubb*$^{-/-}$ embryonic brains can directly contribute to the inhibition of neuronal differentiation and the promotion of glial differentiation.

To confirm that aberrant activation of Notch signaling in *Ubb*$^{-/-}$ cells is responsible for inhibition of neurogenesis and promotion of gliogenesis, expression levels of *Neurog1*, *Fox3* (*NeuN*), and *Gfap* were determined in the presence or absence of DAPT. As expected, *Fox3* (*NeuN*) mRNA levels decreased while *Gfap* mRNA levels increased in *Ubb*$^{-/-}$ cells compared to wild-type cells during the culture period (Fig. 5b). However, upon repression of Notch signaling by DAPT, *Neurog1* and *Fox3* (*NeuN*) mRNA levels increased significantly, while *Gfap* mRNA levels were reduced significantly in *Ubb*$^{-/-}$ cells on DIV13 (Fig. 5b). In addition, a significant reduction of apoptosis was detected in *Ubb*$^{-/-}$ cells during culture in the presence of DAPT (Fig. 5c). Repression of Notch signaling also decreased the number of GFAP$^+$ astrocytes and increased levels of TUJ1$^+$ neurons during the culture period (Fig. 5c and 5d). Based on these results, we conclude that aberrant activation of Notch signaling

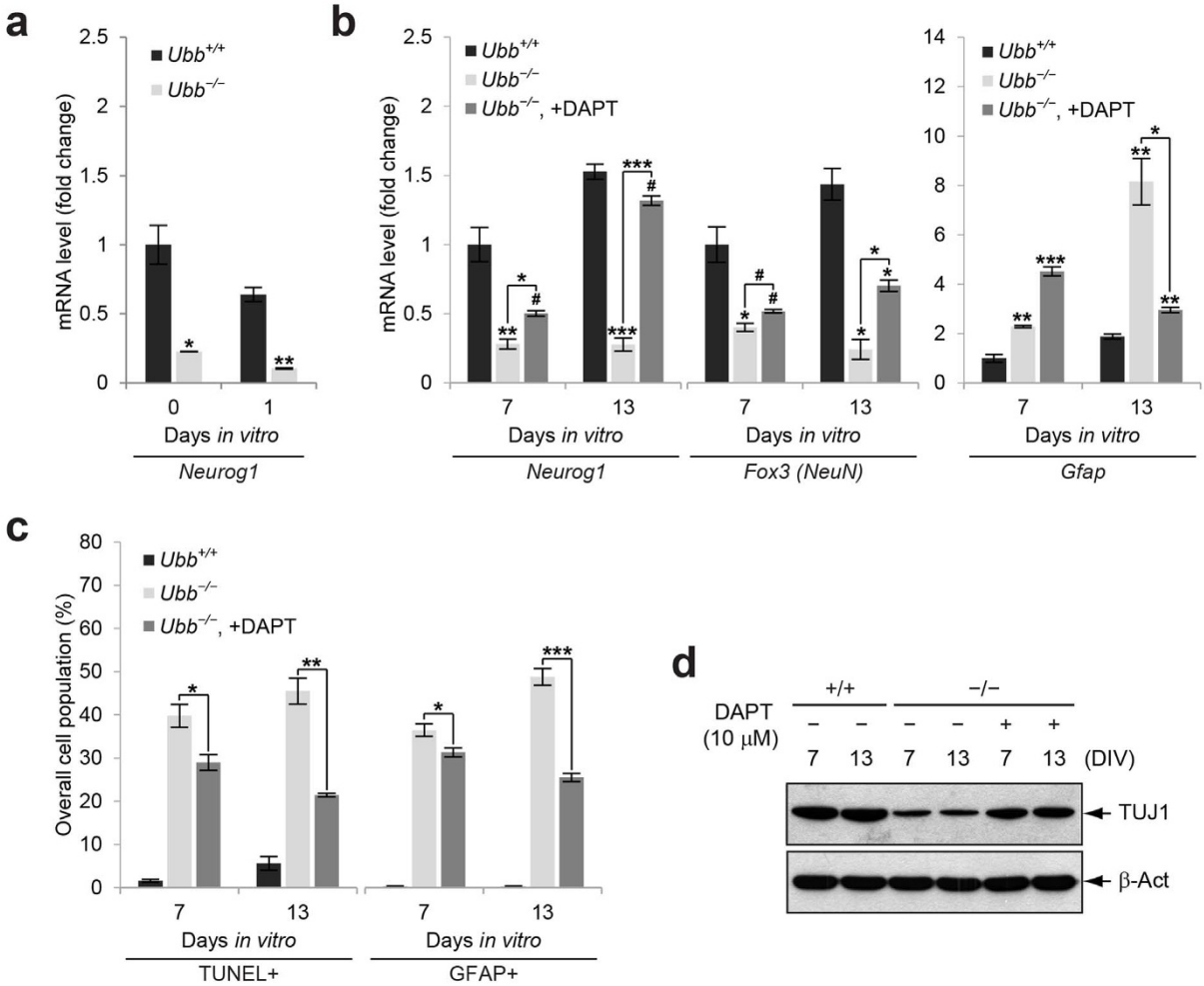

Figure 5 | Improvement of *Ubb*$^{-/-}$ neuronal and glial phenotypes via pharmacological intervention of Notch signaling. (a) Expression levels of the proneuronal gene *Neurog1* in wild-type (*Ubb*$^{+/+}$) and *Ubb*$^{-/-}$ cells ($n = 3$ each) on DIV0 and DIV1 were determined by qRT-PCR as described in Figure 4(a). (b) Expression levels of *Neurog1*, *Fox3* (*NeuN*), and *Gfap* in wild-type (*Ubb*$^{+/+}$) and *Ubb*$^{-/-}$ cells ($n = 3$ each) on DIV7 and DIV13 were determined by qRT-PCR as described in Figure 4(b). DAPT treatment of *Ubb*$^{-/-}$ cells was carried out as described in Figure 4(b). (c) The percentage of apoptotic (TUNEL$^+$) or GFAP$^+$ cells in wild-type (*Ubb*$^{+/+}$), *Ubb*$^{-/-}$, and DAPT-treated *Ubb*$^{-/-}$ cells ($n = 3$ each) on DIV7 and DIV13 was determined in a similar manner as described in Figure 2(a). (d) Immunoblot detection of TUJ1 in wild-type (*Ubb*$^{+/+}$), *Ubb*$^{-/-}$, and DAPT-treated *Ubb*$^{-/-}$ cells on DIV7 and DIV13. β-actin (β-Act) was used as a loading control. Representative immunoblot results of cells from three different embryonic brains per genotype are shown (d), and data are expressed as the means ± SEM from the indicated number of samples (a–c). $^{\#}P < 0.1$; $^{*}P < 0.05$; $^{**}P < 0.01$; $^{***}P < 0.001$ *vs.* *Ubb*$^{+/+}$ on each day or as indicated by bars.

in *Ubb*$^{-/-}$ cells is, at least in part, responsible for dysregulation of NSC differentiation with premature onset of gliogenesis and suppression of neurogenesis.

Discussion

In this study, we showed that cellular Ub pools determine the differentiation of NSCs into neurons or glial cells via regulation of Notch signaling (Fig. 6). In the embryonic stage, Notch signaling is downregulated, promoting neurogenesis and suppressing gliogenesis. In the postnatal stage, Notch signaling is upregulated, which supports gliogenesis and neuronal maturation. Since Notch activation is required for self-renewal or maintenance of NSCs, timely and sustained downregulation of Notch signaling is an essential determinant of neurogenesis during the mid-gestation period[14]. After Notch receptor interacts with its ligand Delta (DLL1) in neighboring cells, Notch signaling is initiated by cleavage of NICD by γ-secretase[23]. Released NICD then migrates into the nucleus and functions as a part of the transactivator complex to promote transcription of Notch target genes. Therefore, timely degradation of NICD is likely important for tight regulation of Notch signaling.

Decreased availability of cellular Ub pools due to disruption of polyubiquitin gene *Ubb* has prevented the timely degradation of NICD, resulting in increased transcription of Notch target genes. Because increased steady-state levels of NICD should definitely contribute to upregulation of Notch target genes, it is suspected that timely downregulation of Notch signaling may not be achieved during mid-gestation when Ub is not readily available, leading to prolonged activation of Notch signaling, which is the major cause of the dysregulated NSC differentiation.

To the best of our knowledge, our study is the first to demonstrate that aberrant activation of Notch signaling due to reduced levels of Ub in cells from mid-gestation embryonic brains can lead to alterations in the fate of NSCs, resulting in the premature onset of gliogenesis and suppression of neurogenesis. Furthermore, our results suggest that aberrant activation of Notch signaling may continue until the postnatal stage in *Ubb*$^{-/-}$ mice. Under high gliogenic potential, astrocytes dramatically increase in number and become reactive after losing neuroprotective functions or after gaining neurotoxic characteristics[23,24]. In fact, pro-inflammatory cytokine levels gradually increased in *Ubb*$^{-/-}$ cells during the culture period (Park et al., unpublished data). Therefore, early-onset reactive gliosis in *Ubb*$^{-/-}$ mice is most likely due to dysregulation of NSC differentiation during brain development resulting from the continued activation of Notch signaling.

Although we cannot completely exclude the possibility that the increased *Notch* expression in *Ubb*$^{-/-}$ cells can also be attributed to the increased astrocyte numbers or to the increased ratio of astrocytes to neurons, the following evidence suggests that this may not be the case. Based on the transcriptome database for astrocytes and neurons isolated from postnatal mouse brains on day 7 (P7), *Gfap* expression is about >100-fold higher in astrocytes than in neurons and *Notch* expression is about 10-fold higher in astrocytes than in neurons[25]. Between DIV0 and DIV1, the fold increases in *Gfap* and *Notch* expression in *Ubb*$^{-/-}$ cells compared to wild-type cells were almost similar (see Fig. 3e and 4a). Therefore, increased *Notch* expression was probably not due to the increased number of astrocytes. Although astrocyte numbers and *Gfap* expression increased dramatically in *Ubb*$^{-/-}$ cells as culture progressed (see Fig. 2f, 5b, and 5c), there was no proportional increase in *Notch* expression (see

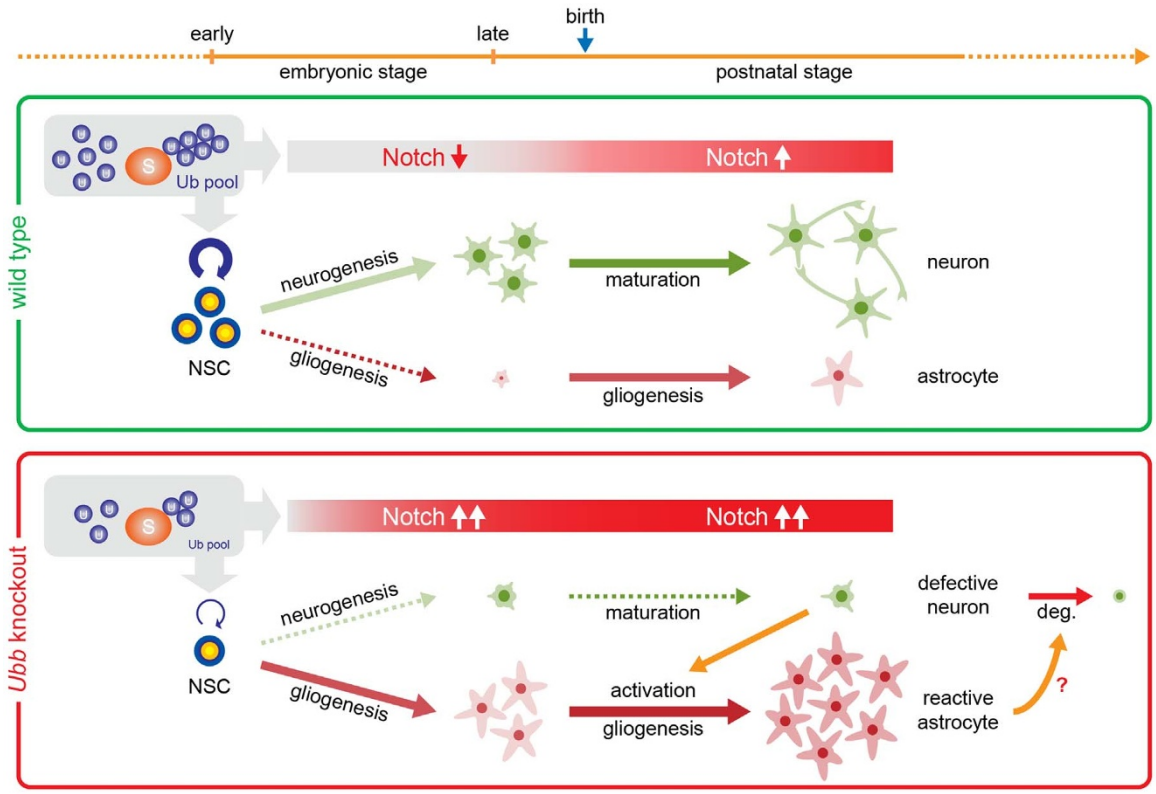

Figure 6 | Proposed model of Ub-dependent neural development via regulation of Notch signaling. Disruption of polyubiquitin gene *Ubb* reduces levels of cellular Ub pools, resulting in prolonged activation of Notch signaling and impaired neural stem cell (NSC) maintenance or self-renewal. Notch activation during the embryonic stage could lead to dysregulation of NSC differentiation with premature gliogenesis and impaired neurogenesis. Defective neurons may be responsible for activation of astrocytes, which probably cause degeneration (deg.) of defective neurons. Detailed descriptions are provided in the Discussion section.

Fig. 4b). Therefore, Notch activation in $Ubb^{-/-}$ embryonic brains and $Ubb^{-/-}$ cells may not be attributed to the presence of astrocytes, but the activation more likely causes premature differentiation of NSCs into astrocytes.

Although Notch activation is required for neuronal maturation, as $Ubb^{-/-}$ neurons were not properly generated during the embryonic stage, defective $Ubb^{-/-}$ neurons may not mature as wild-type neurons (Fig. 6). Defective neurons interact with and activate astrocytes, which, in turn, are responsible for the degeneration of these defective neurons or their progenitors[23]. One possible mechanism for this process is the secretion of lipocalin 2 (LCN2) by reactive astrocytes[24], which exerts specific toxicity on neurons to promote their degeneration. LCN2 has also been known as a mediator of reactive astrocytosis, and its expression is increased when astrocytes are under inflammatory stress or during reactive astrocytosis[26]. LCN2 is also responsible for upregulation of *Gfap*, which occurs during reactive astrocytosis. As *Lcn2* mRNA levels increased dramatically in $Ubb^{-/-}$ cells during the culture period (Park et al., unpublished data), it is highly likely that $Ubb^{-/-}$ astrocytes underwent activation. In fact, adult-onset hypothalamic neurodegeneration in $Ubb^{-/-}$ mice is preceded by neuronal dysfunction in the hypothalamus[7,8]. Therefore, these dysfunctional neurons may be responsible for the activation of astrocytes, even though their numbers are maintained, and the reactive astrocytes may be responsible for adult-onset neurodegeneration in $Ubb^{-/-}$ mice.

It was expected that aberrant activation of Notch signaling in $Ubb^{-/-}$ embryonic brains would enhance proliferation of NSCs. However, our data suggest that the capacity to maintain NSCs may be reduced in $Ubb^{-/-}$ embryonic brains due to reduced proliferation of NSCs. In fact, reduced cellular proliferation capacity is observed in various cell types when cellular Ub pools are reduced, including hematopoietic (stem) cells, fetal liver epithelial progenitor cells, hepatocytes, and mouse embryonic fibroblasts[27–29]. The proliferation capacity of NSCs was also compromised in $Ubb^{-/-}$ embryonic brains, resulting in reduction of NSC numbers.

Expression levels of Notch ligand *Dll1*, Notch target gene *Hes1*, and proneuronal gene *Neurog2* in NSCs have been shown to oscillate (repeated up and downregulation with 2–3 hour intervals) to maintain the status of NSCs before differentiation into neurons[16,30]. In particular, both *Hes1* mRNA and HES1 protein levels oscillate in response to negative autoregulation of *Hes1* transcription and Ub-dependent proteasomal degradation of HES1 protein, respectively[31]. Therefore, timely degradation of HES1, as well as other Notch signaling molecules in oscillations, including NICD, may not be tightly regulated when cellular Ub levels are reduced, resulting in the reduced capacity to maintain NSCs in $Ubb^{-/-}$ embryonic brains. These observations further support the finding that self-renewal or maintenance of NSCs is significantly reduced in $Ubb^{-/-}$ embryonic brains.

In conclusion, our study using cells isolated from mouse embryonic brains suggests that cellular Ub pools play an important role in determining the fate and self-renewal of NSCs. Decreased availability of cellular Ub pools resulted in reduced numbers of NSCs, and these NSCs underwent premature gliogenesis and suppression of neurogenesis due to prolonged activation of Notch signaling, leading to defective neuronal development. Defective neurons may activate astrocytes into reactive astrocytes, resulting in apoptosis in defective neurons or their progenitors, and even resulting in apoptosis in astrocytes. Therefore, our *in vitro* cell culture results support the phenotypes observed in $Ubb^{-/-}$ mice, including reactive gliosis and neurodegeneration[7,8].

Methods

Mouse studies. All mice were maintained in plastic cages with *ad libitum* access to food and water, with a 12-hr light cycle[32]. Wild-type and $Ubb^{-/-}$ embryos were obtained from interbreeding of $Ubb^{+/-(eGFP\text{-}puro)}$ mice. All experiments were performed in accordance with relevant guidelines and regulations approved by the University of Seoul Institutional Animal Care and Use Committee (UOS IACUC). All experimental protocols, including breeding, euthanasia, and dissection of embryonic brains, were approved by the UOS IACUC (approval numbers are UOS-091201-1 and UOS-121025-2).

Primary cell culture. Embryonic brains were dissected from 14.5 days post coitum (dpc) and placed in Ca^{2+} and Mg^{2+}-free Hank's Balanced Salt Solution (HBSS) to remove the cerebellum and meninges. Isolated brains were transferred to trypsinization solution containing 0.05% trypsin/EDTA (Cellgro) and incubated for 30 min at 37°C with vigorous shaking at 250 rpm. Trypsinization was quenched by adding an equal volume of cell culture medium (DMEM supplemented with 10% fetal bovine serum (FBS), 20 mM L-glutamine, and 1% antibiotics/antimycotics (Cellgro)). After centrifugation at 1,000 rpm for 5 min, the tissue was triturated in neuronal cell culture medium (Neurobasal® medium supplemented with B-27® supplement (Invitrogen), 1× GlutaMax, 0.5 mM L-glutamine, and 1% antibiotics/antimycotics (Cellgro)) by gentle pipetting through a 1000 μl pipette tip. Triturated tissues were strained through a 40 μm nylon mesh. Resulting cells were plated on a tissue culture dish coated with poly-D-lysine (MW 30,000–70,000, Sigma-Aldrich) and laminin (Invitrogen) at 1×10^4 to 1.5×10^5 cells/cm^2 depending on the experiment, and then cultured in the same medium. One-half of the medium was changed every three days.

Immunofluorescence analysis and TUNEL assay. For immunofluorescence, cells grown on poly-D-lysine-coated coverslips were fixed in 4% paraformaldehyde for 10 min at room temperature (RT), permeabilized with 0.3% Triton X-100/PBS, and blocked with 3% BSA/PBS for 1 hr at RT. Fixed cells were incubated with anti-GFAP (1 : 1,000, Millipore), anti-NeuN (1 : 200, Millipore), anti-NES (1 : 1,000, Abcam) or anti-PH3 (1 : 200, Millipore) antibody at 4°C overnight, washed with PBS, and incubated with Alexa Fluor 488-conjugated goat anti-mouse IgG or Alexa Fluor 555-conjugated donkey anti-rabbit IgG (1 : 1,000, Invitrogen) along with 0.1 μg/ml of DAPI for 1 hr at RT. Cells were then mounted using Prolong Gold antifade reagent (Invitrogen). Images were visualized with a Carl Zeiss AxioImager A2 microscope or Carl Zeiss Axiovert 200 M microscope equipped with a confocal laser scanning module LSM510. Immunofluorescence analysis of frozen embryonic brain sections was carried out as previously described[29]. Sagittal embryonic brain sections were incubated with anti-NES (1 : 200, Abcam) or anti-GFAP antibody (1 : 200, Millipore), followed by Alexa Fluor 555-conjugated goat anti-mouse IgG (1 : 200, Invitrogen) along with 0.1 μg/ml of DAPI. Apoptotic cells were detected by TUNEL assay using an ApopTag® red *in situ* apoptosis detection kit according to the manufacturer's protocol (Millipore).

Immunoblot analysis. For immunoblot analysis, cell lysates were prepared in hypotonic buffer and processed as previously described[28]. Briefly, total cell lysates (15 μg) were subjected to SDS-PAGE, followed by immunoblot detection with anti-TUJ1 (1 : 1,000, Millipore), anti-GFAP (1 : 1,000, Millipore), anti-NeuN (1 : 500, Millipore), anti-CASP3 (1 : 3,000, Cell Signaling), anti-Notch3 (1 : 200, Santa Cruz Biotechnology), or anti-β-actin antibody (1 : 10,000, Sigma-Aldrich). Based on the types of primary antibodies, the appropriate HRP-conjugated goat anti-mouse or anti-rabbit IgG (1 : 10,000, Enzo Life Sciences) or HRP-conjugated donkey anti-goat IgG (1 : 5,000, Santa Cruz Biotechnology) was used.

Quantitative real-time RT-PCR. Quantitative real-time RT-PCR (qRT-PCR) was carried out essentially as previously described with slight modifications[28]. Briefly, total RNA was isolated from cells using an RNeasy kit (Qiagen), and 10 ng of total RNA was used as a template for reverse transcription using the GoScript™ Reverse Transcription System (Promega). For qRT-PCR, we used an EvaGreen qPCR Mastermix-iCycler kit (Applied Biological Materials) and iCycler system (Bio-Rad). The mRNA expression levels of *Gfap*, *Fox3*, *Nes*, *Notch1*, *Hes5*, *Hey1*, and *Neurog1* were normalized to the level of *Gapdh*. Primers used for qRT-PCR are as follows: *Gfap*-F (5′-CGA GTC CCT AGA GCG GCA AAT G-3′); *Gfap*-R (5′-GTA GGT GGC GAT CTC GAT GTC-3); *Fox3*-F (5′-CCA GGC ACT GAG GCC AGC ACA CAG C-3′); *Fox3*-R (5′-CTC CGT GGG GTC GGA AGG GTG G-3′); *Nes*-F (5′-GAA GCC CTG GAG CAG GAG AAG CA-3′); *Nes*-R (5′-TCC AGG TGT CTG CAA CCG AGA GTT C-3′); *Notch1*-F (5′- GTG TCG TGT GTC AAG CTG ATG-3′); *Notch1*-R (5′- CAT CCT GGG TTG TGC TCT TAG-3′); *Hes5*-F (5′-GCA GCA TAG AGC AGC TGA AG-3′); *Hes5*-R (5′-AGG CTT TGC TGT GTT TCA GG-3′); *Hey1*-F (5′-AAA ATG CTG CAC ACT GCA GG-3′); *Hey1*-R (5′-CGA GTC CTT CAA TGA TGC TCA G-3′); *Neurog1*-F (5′-ACC TGT CCA GCT TCC TCA CC-3′); *Neurog1*-R (5′-GTT CCT GCT CTT CGT CCT G-3′); *Gapdh*-F (5′-GGC ATT GCT CTC AAT GAC AA-3′); *Gapdh*-R (CTT GCT CAG TGT CCT TGC TG-3′).

Statistical analysis. Two-tailed unpaired Student's *t*-tests or two-way analysis of variance (ANOVA) with the Holm-Sidak method were used to compare the data between experimental and control groups. Although $P < 0.05$ was considered to be statistically significant in most cases, $P < 0.1$ was also noted in certain cases.

1. Hershko, A. & Ciechanover, A. The ubiquitin system. *Annu. Rev. Biochem.* **67**, 425–479 (1998).
2. Hochstrasser, M. Ubiquitin-dependent protein degradation. *Annu. Rev. Genet.* **30**, 405–439 (1996).

3. Ravid, T. & Hochstrasser, M. Diversity of degradation signals in the ubiquitin-proteasome system. *Nat. Rev. Mol. Cell Biol.* **9**, 679–690 (2008).
4. Wilkinson, K. D. *et al.* The neuron-specific protein PGP 9.5 is a ubiquitin carboxyl-terminal hydrolase. *Science* **246**, 670–673 (1989).
5. Kawabe, H. & Brose, N. The role of ubiquitylation in nerve cell development. *Nat. Rev. Neurosci.* **12**, 251–268 (2011).
6. Tai, H. C. & Schuman, E. M. Ubiquitin, the proteasome and protein degradation in neuronal function and dysfunction. *Nat. Rev. Neurosci.* **9**, 826–838 (2008).
7. Ryu, K. Y. *et al.* Loss of polyubiquitin gene *Ubb* leads to metabolic and sleep abnormalities in mice. *Neuropathol. Appl. Neurobiol.* **36**, 285–299 (2010).
8. Ryu, K. Y., Garza, J. C., Lu, X. Y., Barsh, G. S. & Kopito, R. R. Hypothalamic neurodegeneration and adult-onset obesity in mice lacking the *Ubb* polyubiquitin gene. *Proc. Natl. Acad. Sci. USA* **105**, 4016–4021 (2008).
9. Davis, A. A. & Temple, S. A self-renewing multipotential stem cell in embryonic rat cerebral cortex. *Nature* **372**, 263–266 (1994).
10. Gage, F. H. Mammalian neural stem cells. *Science* **287**, 1433–1438 (2000).
11. McKay, R. Stem cells in the central nervous system. *Science* **276**, 66–71 (1997).
12. Qian, X. *et al.* Timing of CNS cell generation: a programmed sequence of neuron and glial cell production from isolated murine cortical stem cells. *Neuron* **28**, 69–80 (2000).
13. Temple, S. The development of neural stem cells. *Nature* **414**, 112–117 (2001).
14. Pierfelice, T., Alberi, L. & Gaiano, N. Notch in the vertebrate nervous system: an old dog with new tricks. *Neuron* **69**, 840–855 (2011).
15. Yoon, K. & Gaiano, N. Notch signaling in the mammalian central nervous system: insights from mouse mutants. *Nat. Neurosci.* **8**, 709–715 (2005).
16. Kageyama, R., Ohtsuka, T., Shimojo, H. & Imayoshi, I. Dynamic regulation of Notch signaling in neural progenitor cells. *Curr. Opin. Cell Biol.* **21**, 733–740 (2009).
17. Kim, K. K., Adelstein, R. S. & Kawamoto, S. Identification of neuronal nuclei (NeuN) as Fox-3, a new member of the Fox-1 gene family of splicing factors. *J. Biol. Chem.* **284**, 31052–31061 (2009).
18. Bilang-Bleuel, A. *et al.* Psychological stress increases histone H3 phosphorylation in adult dentate gyrus granule neurons: involvement in a glucocorticoid receptor-dependent behavioural response. *Eur. J. Neurosci.* **22**, 1691–1700 (2005).
19. Prigent, C. & Dimitrov, S. Phosphorylation of serine 10 in histone H3, what for? *J. Cell Sci.* **116**, 3677–3685 (2003).
20. Itoh, M. *et al.* Mind bomb is a ubiquitin ligase that is essential for efficient activation of Notch signaling by Delta. *Dev. Cell* **4**, 67–82 (2003).
21. Yoon, K. J. *et al.* Mind bomb 1-expressing intermediate progenitors generate notch signaling to maintain radial glial cells. *Neuron* **58**, 519–531 (2008).
22. Kageyama, R., Ohtsuka, T. & Kobayashi, T. Roles of *Hes* genes in neural development. *Dev. Growth Differ.* **50 Suppl 1**, S97–103 (2008).
23. Ables, J. L., Breunig, J. J., Eisch, A. J. & Rakic, P. Not(ch) just development: Notch signalling in the adult brain. *Nat. Rev. Neurosci.* **12**, 269–283 (2011).
24. Bi, F. *et al.* Reactive astrocytes secrete lcn2 to promote neuron death. *Proc. Natl. Acad. Sci. USA* **110**, 4069–4074 (2013).
25. Cahoy, J. D. *et al.* A transcriptome database for astrocytes, neurons, and oligodendrocytes: a new resource for understanding brain development and function. *J. Neurosci.* **28**, 264–278 (2008).
26. Lee, S. *et al.* Lipocalin-2 is an autocrine mediator of reactive astrocytosis. *J. Neurosci.* **29**, 234–249 (2009).
27. Park, H., Yoon, M. S. & Ryu, K. Y. Disruption of polyubiquitin gene *Ubc* leads to defective proliferation of hepatocytes and bipotent fetal liver epithelial progenitor cells. *Biochem. Biophys. Res. Commun.* **435**, 434–440 (2013).
28. Ryu, K. Y. *et al.* The mouse polyubiquitin gene *UbC* is essential for fetal liver development, cell-cycle progression and stress tolerance. *EMBO J.* **26**, 2693–2706 (2007).
29. Ryu, K. Y., Park, H., Rossi, D. J., Weissman, I. L. & Kopito, R. R. Perturbation of the hematopoietic system during embryonic liver development due to disruption of polyubiquitin gene *Ubc* in mice. *PLoS ONE* **7**, e32956 (2012).
30. Shimojo, H., Ohtsuka, T. & Kageyama, R. Oscillations in notch signaling regulate maintenance of neural progenitors. *Neuron* **58**, 52–64 (2008).
31. Hirata, H. *et al.* Oscillatory expression of the bHLH factor Hes1 regulated by a negative feedback loop. *Science* **298**, 840–843 (2002).
32. Ryu, K. Y. *et al.* The mouse polyubiquitin gene *Ubb* is essential for meiotic progression. *Mol. Cell. Biol.* **28**, 1136–1146 (2008).

Acknowledgments

This study was supported by a grant from the Korean Health Technology R&D Project, Ministry of Health & Welfare, Republic of Korea (A111485) to K.-Y.R.

Author contributions

H.-W.R. and K.-Y.R. conceived and designed the research. H.-W.R. and C.-W.P. performed the experiments and analyzed the data. H.-W.R. and K.-Y.R. wrote the paper.

Additional information

Supplementary information accompanies this paper at http://www.nature.com/scientificreports

Competing financial interests: The authors declare no competing financial interests.

How to cite this article: Ryu, H.-W., Park, C.-W. & Ryu, K.-Y. Disruption of polyubiquitin gene *Ubb* causes dysregulation of neural stem cell differentiation with premature gliogenesis. *Sci. Rep.* **4**, 7026; DOI:10.1038/srep07026 (2014).